Astronomy & Astrophysics manuscript no.
(will be inserted by hand later)

The Sagittarius dwarf irregular galaxy: metallicity and stellar populations ⋆

Y. Momany[1,2], E. V. Held[3], I. Saviane[4], and L. Rizzi[3,2]

[1] European Southern Observatory, Karl-Schwarschild-Str. 2, D-85748 Garching, Germany
[2] Dipartimento di Astronomia, Università di Padova, vicolo dell'Osservatorio 2, I–35122 Padova, Italy
e-mail: momany@pd.astro.it
[3] Osservatorio Astronomico di Padova, vicolo dell'Osservatorio 5, I–35122 Padova, Italy e-mail: (held,rizzi)@pd.astro.it
[4] European Southern Observatory, Casilla 19001, Santiago 19, Chile e-mail: isaviane@eso.org

Abstract. We present deep BVI observations of the dwarf irregular galaxy UKS1927-177 in Sagittarius (SagDIG). Statistically cleaned V, $(B-I)$ color-magnitude diagrams clearly display the key evolutionary features in this galaxy. Previously detected C stars are located in the color-magnitude diagrams and shown to be variable, thus confirming the presence of a significant upper-AGB intermediate age population. A group of likely red supergiants is also identified, whose magnitude and color is consistent with a 30 Myr old burst of star formation. The observed colors of both blue and red stars in SagDIG are best explained by introducing a differential reddening scenario in which internal dust extinction affects the star forming regions. Adopting a low reddening for the red giants, $E(B-V) = 0.07 \pm 0.02$, gives [Fe/H]$=-2.1 \pm 0.2$ for the mean stellar metallicity, a value consistent with the [O/H] abundance measured in the HII regions. This revised metallicity, which is in accord with the trend of metallicity against luminosity for dwarf irregular galaxies, is indicative of a "normal", although metal-poor, dIrr galaxy. A quantitative description is given of the spatial distribution of stars in different age intervals, in comparison with the distribution of the neutral hydrogen. We find that the youngest stars are located near the major peaks of emission on the HI shell, whereas the red giants and intermediate-age C stars define an extended halo or disk with scale length comparable to the size of the hydrogen cloud. The relationship between the distribution of ISM and star formation is briefly discussed.

Key words. Galaxies: fundamental parameters – SagDIG – Local Group – stellar populations – star formation history.

1. Introduction

The Sagittarius dwarf irregular (dIrr) galaxy, also known as SagDIG or UKS 1927-177, is a quite difficult object to study because of its low Galactic latitude and consequent high foreground contamination. First reported by Cesarsky et al. (1977) on ESO Schmidt photographic plates, the galaxy was studied by Longmore et al. (1978), who derived a total luminosity $M_B = -10.5$. The first CCD study of the resolved star content in SagDig was that of Cook (1987; hereafter C87), who obtained both intermediate-band and broad-band photometry. Recently, two new investigations have improved our knowledge of the distance and stellar content of this galaxy (Karachentsev et al. 1999; Lee & Kim 2000; hereafter KAM99 and LK00 respectively). A new distance modulus was derived from the tip of the RGB, equal to $(m-M)_0 = 25.13$ in KAM99 and $(m-M)_0 = 25.36$ in LK00, respectively. This distance indicates that SagDIG is a member of the Local Group (LG), confirming the evidence from its negative radial velocity and position in the $V_\odot$ *vs.* $\cos\theta$ diagram (van den Bergh 1994; Pritchet & van den Bergh 1999). Both studies, while adopting different estimates for the reddening, concluded that SagDIG has the lowest metallicity among the LG star forming dwarf galaxies (KAM99 estimated [Fe/H]~ -2.45, while LK00 give [Fe/H] in the range -2.8 to -2.4; both estimates are based on an extrapolation of the calibration relation for Galactic globular clusters).

The cold and warm interstellar medium (ISM) of SagDIG and its kinematics have been the subject of several investigations. Skillman et al. (1989b) obtained optical spectrophotometry of the most luminous HII regions, and estimated a [O/H] abundance $\sim$ 3% of the solar value. New measurements of the O and N abundance

Send offprint requests to: Y. Momany
⋆ Based on data collected at the European Southern Observatory, La Silla, Chile, prop. No. 63.N-0024

in the HII regions of SagDIG are presented in a companion paper (Saviane et al. 2001). The new estimate, $12+\log(O/H) = 7.23\pm0.20$, is by 0.2 dex more metal-poor than found by Skillman et al. (1989b). The photometric properties of the HII regions were investigated by Strobel et al. (1991), who detected 3 regions in their 2′.5 square field.

High-resolution, high sensitivity VLA observations of the SagDIG HI content have been obtained by Young & Lo (1997) (see also Lo et al. 1993). About $1.2\times10^7\ M_\odot$ of H+He have been estimated (using the new distance from KAM99 and the HI mass from Young & Lo), distributed in an almost symmetric ring likely produced by the combined effects of stellar winds and supernovae. SagDIG thus appears to have a high mass fraction in the form of neutral gas, $M_{HI}/L_B = 1.6$, a value quite typical of the HI content in dwarf irregular galaxies (see Mateo 1998).

Because of its high gas content, low luminosity, and especially its claimed very low metallicity, SagDIG may be a clue to the origin and evolution of dwarf galaxies. Although located at the border of the Local Group it is still close enough to allow us to study both its stellar populations and the gaseous component, and to compare their physical properties. In particular, a sound knowledge of the metallicity of SagDIG is important to constrain the luminosity-metallicity relation for dIrrs at the metal-poor end, and to trace the metal enrichment history in dwarf galaxies. All this motivated an independent study of the metallicity, distance, and stellar content of SagDIG. The large baseline provided by the $(B-I)$ color, together with an analysis based on statistical subtraction of the Galactic foreground, allowed us to improve the discrimination of young and old stellar populations in the color-magnitude diagram (CMD). By accounting for the differential effects of internal dust extinction, we revise upward the [Fe/H] estimate and show that the metal abundances of the red stars and the ISM can be easily reconciled.

The plan of the paper is as follows. In Sect. 2 we present the data reduction and calibration. Section 3 presents color-magnitude diagram in different colors, using a statistical correction of the foreground contamination. The CMD location of C stars is also discussed. In Sect. 4 we rederive the distance and metallicity of SagDIG by assuming a different reddening for the young and old populations. The properties and different spatial distributions of the blue and red stellar populations are quantified and discussed in Sect. 5, where the surface density of young stars in different age intervals is compared with the projected distribution of neutral hydrogen. As a result of the revised metallicity, SagDIG is shown to fit well the known luminosity-abundance trend of dwarf irregular galaxies. Our results are summarized in Sect. 6.

2. Observations and data reduction

Observations of the Sagittarius dwarf irregular were obtained in two runs. SagDIG was first observed on the photometric night of Sept. 8, 1996, using EFOSC2 at the ESO/MPI 2.2m telescope. The EFOSC2 camera was equipped with a 2048×2048 Loral CCD, with pixel size of 0″.26. A readout window was employed to discard the vignetted edges of the CCD, yielding a useful area of $6'.9\times6'.9$. Since the tidal radius of SagDig is only $\sim 1'.7$ (Mateo 1998), no observations of a separate control field were needed. A detailed account of the observations and reduction for this run can be found in our study of the Phoenix dSph/dI galaxy (Held et al. 1999). The galaxy was re-observed in better seeing conditions on the night of 30 Sept. 1999 with the EMMI multi-mode instrument on the ESO NTT telescope. The sky was marginally photometric with occasionally some thin cirrus. The total exposure times were 1^h in V, 20^m in B, and 40^m in I. The V and I data were obtained using a 2048×2048 Tektronix CCD at the red arm of EMMI, with pixel size of 0.24 μm (0″.27) and a field of view of $9'.2\times9'.2$. The B images were taken at the blue arm of EMMI, with a 1024×1024 Tektronix CCD with a projected pixel size of 0″.37 and a smaller field-of-view, $6'.2\times6'.2$. The observing log for both runs is given in Tab. 1.

Table 1. The journal of observations

Night	Tel.	Filter	$t_{\rm exp}[s]$	X	FWHM
Sept. 8, 1996	2.2m	B	2×900	1.02	1″.3
Sept. 8, 1996	2.2m	V	2×600	1.05	1″.5
Sept. 8, 1996	2.2m	I	2×900	1.03	1″.4
Sept. 30, 1999	NTT	B	4×300	1.08	1″.0
Sept. 30, 1999	NTT	V	12×300	1.08	1″.0
Sept. 30, 1999	NTT	I	8×300	1.16	0″.9

The processing of the images was carried out within both the IRAF and MIDAS environments. After bias subtraction and flat-fielding (using twilight sky flats) all images were registered, and sum images were produced for each telescope by co-adding all images taken with the same filter. The programs DAOPHOT II /ALLSTAR (Stetson 1987) were run on the sum images to obtain stellar photometry by point spread function (PSF) fitting. For the NTT data, we also used the ALLFRAME program (Stetson 1994), which combines PSF photometry carried out on the individual images. The 2.2m data set was mainly employed for calibration.

Calibration of the 2.2m data was based on observations of standard star fields from Landolt (1992). The calibration procedure and color transformations are identical to those described in Held et al. (1999). The total zero point errors, including the uncertainties in the calibrations, are 0.012, 0.013, and 0.013 mag in B, V, and I, respectively.

The NTT data were independently calibrated using the relations:

$$B = b' - 0.126\,(B-V) + 24.890 \quad (1)$$

$$V = v' + 0.017\,(B-V) + 25.113 \quad (2)$$

$$V = v' + 0.017\,(V-I) + 25.113 \quad (3)$$

Table 2. The photometric errors (1σ) and completeness from the artificial star experiments

BVI	σ_B	σ_V	σ_I	C_B	C_V	C_I
18.8	0.01	0.01	0.01	0.998	0.998	0.994
19.3	0.01	0.01	0.01	0.999	0.997	0.994
19.8	0.01	0.01	0.02	0.997	0.997	0.990
20.3	0.01	0.02	0.02	0.997	0.995	0.990
20.8	0.01	0.02	0.03	0.992	0.994	0.985
21.3	0.02	0.03	0.05	0.992	0.989	0.980
21.8	0.02	0.04	0.06	0.994	0.984	0.970
22.3	0.03	0.05	0.08	0.985	0.975	0.945
22.8	0.04	0.07	0.12	0.984	0.963	0.880
23.3	0.06	0.10	0.15	0.967	0.920	0.825
23.8	0.08	0.12	0.17	0.956	0.860	0.669
24.3	0.10	0.13	0.19	0.940	0.670	0.450
24.8	0.12	0.17	0.23	0.760	0.450	0.278
25.3	0.18	0.21	0.26	0.550	0.255	0.196

$$I = i' - 0.021\,(V-I) + 24.411 \quad (4)$$

where the b', v', and i' magnitudes are the instrumental magnitudes for the standard stars, measured in apertures with radius $6''.9$, normalized to zero airmass and 1 s exposure. The instrumental PSF magnitudes of stars in the SagDIG field were converted to normalized aperture magnitudes using a growth curve analysis of bright isolated stars in the individual images (see Saviane et al. 1996). A comparison of stars in common with the 2.2m data set gives the following median zero point differences: ΔB (2.2m–NTT) $= -0.02$, $\Delta V = 0.01$, and $\Delta I = -0.05$. The magnitude scales are therefore in good agreement, especially for the B and V bands. Since the 2.2m data have well established calibration zero points, the latter were adopted as the reference photometric scale. Small adjustments were applied to the NTT data accordingly.

Photometric errors and the completeness were estimated from artificial star experiments. Simulated stars were added to the sum images by randomly distributing them around the nodes of a grid of triangles – a procedure well suited to prevent self-crowding (see Saviane et al. 2000). The frames were then reduced and calibrated as done for the original images. A comparison of the input and measured magnitudes for the retrieved stars gives the internal errors (rms in 0.5 mag bins) and completeness, which are given in Tab. 2.

Calibrated magnitudes for the stars in the SagDIG field were compared with previous photometry to check the reliability of the zero points. Our results agree with previous data of C87. The median differences are $\Delta V = V_{us} - V_{C87} = 0.020 \pm 0.024$, and $\Delta(V-I) = 0.030 \pm 0.023$ (the errors being standard deviations of the residuals). A direct comparison is not possible with the data of KAM99, since photometric catalogs have not been published. However, the magnitudes and colors of key features in their CMDs (such as the RGB tip or the blue plume) are in excellent agreement with those measured in our diagrams. The $(V-I)$ colors measured by LK00 and by us show significant disagreement, the median shift being $\Delta(V-I) = 0.220 \pm 0.086$ (this paper − LK00). The blue shift in the $(V-I)$ scale of LK00 significantly affects their metallicity estimate. A systematic difference is also present in $(B-V)$ colors, $\Delta(B-V) = 0.100 \pm 0.065$ (us – LK00). The V magnitude scales are more nearly consistent, yielding $\Delta V = -0.040 \pm 0.069$.

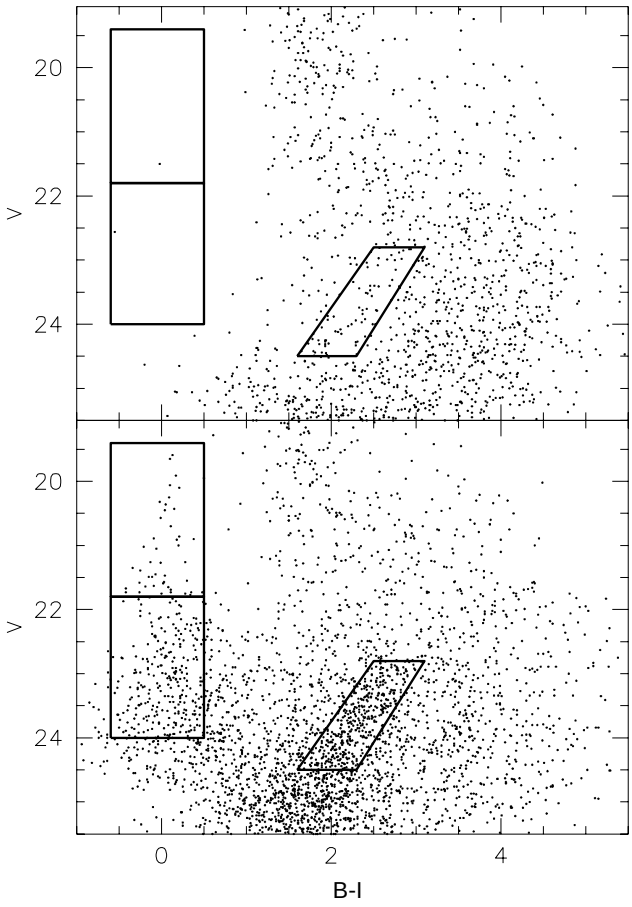

Fig. 1. The V, $(B-I)$ color-magnitude diagram of a field centered on SagDIG (*lower panel*), compared with the CMD in the control region (*upper panel*). Both the inner and outer region have an area $5'.5 \times 2'.7$. Blue and red stars belonging to the galaxy, in excess over the foreground contamination, are clearly visible in the diagram of the inner region. The rectangles delimit two samples of young stars in two different age intervals, while the slanted box outlines a high-probability sample of red giant stars.

3. The color-magnitude diagrams

The color-magnitude diagram of the inner part of our image, comprising most of the Sagittarius dIrr galaxy, is shown in Fig. 1 (lower panel). The inner region was defined as a $5'.5 \times 2'.7$ rectangle around SagDIG, with the long side in the EW direction, and contains both SagDIG's and

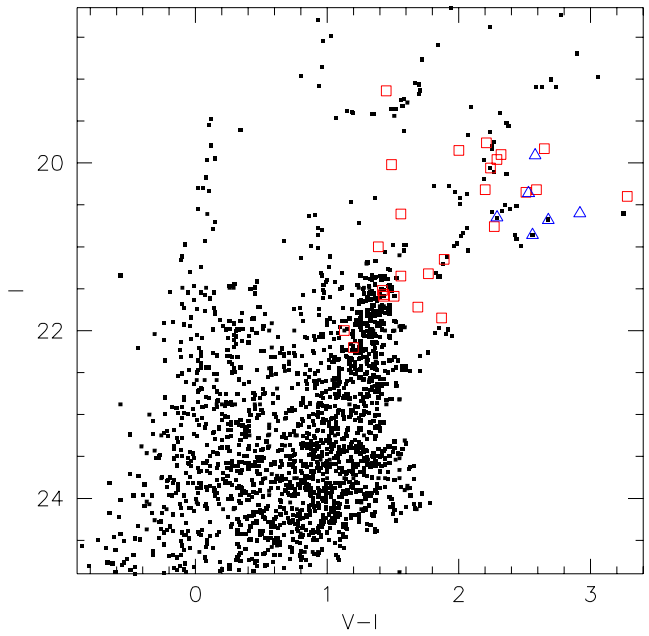

Fig. 2. The I, $(V-I)$ color-magnitude diagram of SagDIG after applying statistical decontamination. We have superimposed the C star candidates found by Cook (1987; *open squares*) and those identified by Demers & Battinelli (2001; *open triangles*).

foreground stars. The CMD of an outer region of equal area (upper panel) illustrates the considerable foreground contribution of stars in the Galactic bulge in the direction of SagDIG. Despite the field contamination, the blue plume of young stars and the red giant branch of SagDIG are evident in the diagram of the inner area. Three CMD regions used to select samples of stars of different ages are outlined in Fig. 1 – these will be utilized in Sect. 5 to study the stellar population gradients in the galaxy.

A statistical foreground subtraction procedure was applied to the analysis of the CMDs of SagDIG. All stars in the CMD of the inner region having a counterpart in the diagram of the outer field were statistically identified as interlopers and culled out. The coincidence was tested in CMD cells 0.3×0.3 mag in color and magnitude, respectively. An example of the cleaned CMD of SagDIG is shown in Fig. 2 (see also Fig. 4).

All evolutionary features are more clearly seen in the decontaminated diagrams than in the raw CMDs. The blue plume of young stars is well delineated for more than 4 mag, and the red giant branch shows a well-defined cutoff and extends over a ~ 3 mag interval in both V and I. Several stars populate the Hertzsprung gap. Although many are likely to be He-burning stars in SagDIG, a fraction of them are possible artifacts caused by the significant crowding in ground-based data.

Two features are noted in all of our statistically decontaminated diagrams, so that they are likely to be real. The first is a group of probable red supergiants located ~ 2 mag above the RGB tip (Fig. 2). The second feature is a tail of very red stars with $V \sim 22$, $V-I \gtrsim 1.5$, strongly resembling the extended tail of intermediate-age asymptotic giant branch (AGB) stars found in many dwarf galaxies. This feature suggests the presence of a significant intermediate-age population.

This conclusion is supported by the remarkable coincidence in magnitude and color with the candidate C stars found by Cook (1987) and more recently by Demers & Battinelli (2001) (see Fig. 2). The C star candidates were classified by Cook (1987) in two groups: a luminous 1 Gyr old population (reaching ~ 2 mag in I above the RGB tip) and a bluer, less luminous population about 10 Gyr old. The comparison between old and new measurements reveals an intrinsic variability of these stars. The cross-identification of C stars is firm, being based on positional coincidence within ± 1 pixel ($0\farcs3$). The differences between Cook's measurements and ours for candidate C stars is, after applying a 2σ clipping, ΔV(this paper-Cook)$= 0.23$ mag with a standard deviation 0.21 mag. This scatter is significantly larger than instrumental errors determined from artificial star experiments (see Tab. 2). Also, it is larger than the standard error of the residuals for the general sample of stars in the same CMD region, for which we measured a mean difference 0.02 mag (us−Cook), with a standard deviation $\sigma_V = 0.09$.

4. Basic properties of SagDIG

In view of the direct dependence of the inferred galaxy distance and metallicity on the adopted E_{B-V}, before discussing the basic properties of SagDIG we must consider in some detail the reddening of this galaxy.

4.1. Foreground and internal extinction

Cook (1987) estimated a relatively low reddening in the direction of SagDIG ($E_{B-V} = 0.07$) from the color distribution of the Galactic foreground stars. This result agrees with the prediction from the HI maps of Burstein & Heiles (1984), $E_{B-V} = 0.08 \pm 0.03$. The infrared dust emission maps of Schlegel et al. (1998) suggest a slightly higher reddening ($E_{B-V} = 0.12 \pm 0.01$). Lee & Kim (2000) used their $(B-V)$, $(V-I)$ two-color diagram to infer a very low reddening for the red giant stars in SagDIG. Reddening values estimated using these colors, however, are poorly constrained because the reddening vector is nearly parallel to the stellar sequence. Following Cook (1987), we have evaluated the extinction in the direction of SagDIG by comparing the $(V-I)$ color distribution of the foreground Galactic stars in our database, brighter than V=22 and redder than $B-I = 0.5$, with the colors of stars in the South Polar Cap (Caldwell & Schecter 1996). The best fit of the two color distributions (particularly of the blue cutoff at $V-I \sim 0.65$ related to the main sequence turnoff of Galactic disk stars) was obtained by assuming a foreground reddening $E(B-V) = 0.07$, with an uncertainty of about ± 0.02 mag. A similar value, $E(B-V) \approx 0.05$, was

obtained by Demers & Battinelli (2001) from the $(R-I)$ distribution of foreground stars.

Evidence for a higher reddening has been found in the star forming regions. In their spectroscopic study of HII regions in SagDIG, Skillman et al. (1989b) obtained $c(\mathrm{H}\beta) = 0.33$. This value was converted into $E_{B-V} = 0.22$ using the relation $c(\mathrm{H}\beta) = 1.47 \times E_{B-V}$ (Seaton 1979). Recent measurements of the Balmer decrement in the largest HII region by Saviane et al. (2001) confirms this high reddening, yielding $E(B-V) = 0.19 \pm 0.04$. While this result strictly pertains to the warm ISM, it is likely to apply also to the young stars in the blue plume, physically associated to the interstellar gas.

The presence of a differential extinction between young and old stars is well known in starburst galaxies (e.g., Calzetti et al. 1994). Recently formed stars are embedded in regions of high dust content, while old stars are distributed in more extended morphological structures (halos or disks) (e.g., Zijlstra & Minniti 1999). A differential reddening has been suggested in some other dIrrs, for instance IC 10 (Sakai et al. 1999). This might well be the case also for SagDIG, where the young stars are concentrated near the HI density peaks (see Sect. 5.2), while the older stars show an extended distribution.

4.2. Distance and metallicity

The I-band magnitude distribution (hereafter LF) of the red giant stars in SagDIG was obtained from a statistically decontaminated sample of stars selected outside a radius $r = 0\farcm9$ from the galaxy center. This choice excluded most star-forming regions, yielding a clean subsample of red giants in the "halo" of SagDIG (Fig. 3). The LF was derived by simply counting stars in the color range $0.8 < V-I < 1.8$.

The clear RGB cutoff seen in the LF was identified as the tip of the red giant branch, and employed to derive the distance to SagDIG according to the iterative methods of Mould & Kristian (1986) and Lee et al. (1993) (see Held et al. 1999). The RGB tip location was measured by filtering the luminosity function with a Sobel kernel (see, e.g., Madore & Freedman 1998 and references therein). This method yielded $I_{\rm tip} = 21.30 \pm 0.15$, where the uncertainty includes the internal error (assumed to be half the bin size) and the calibration errors. As a check, we also measured the RGB cutoff by fitting an error-convolved step function to the magnitude distribution, obtaining the same result. Our estimate of the tip level is therefore slightly brighter than that obtained by KAM99 ($I_{\rm tip} = 21.38$), although the difference is within the quoted errors.

The initial guess of the distance was based on the assumption that $M_I^{\rm RGBT} = -4.0$, which is an excellent approximation for metal-poor systems, where the I luminosity of the RGB tip shows only a modest dependence on the galaxy metallicity (see also Salaris & Cassisi 1998; Bellazzini et al. 2001). Our distance estimate assumes a low reddening ($E_{B-V} = 0.07 \pm 0.05$, $E_{V-I} = 0.09 \pm 0.06$, $A_I = 0.13 \pm 0.10$) for the RGB population, and a mean metallicity [Fe/H]$=-2.08 \pm 0.20$ dex (see below). With these assumptions, we obtained a corrected distance modulus $(m-M)_0 = 25.14 \pm 0.18$ (1.07 ± 0.09 Mpc), a value confirming previous estimates. The distance error includes all uncertainties on the RGB tip magnitude, reddening and metallicity through standard error propagation.

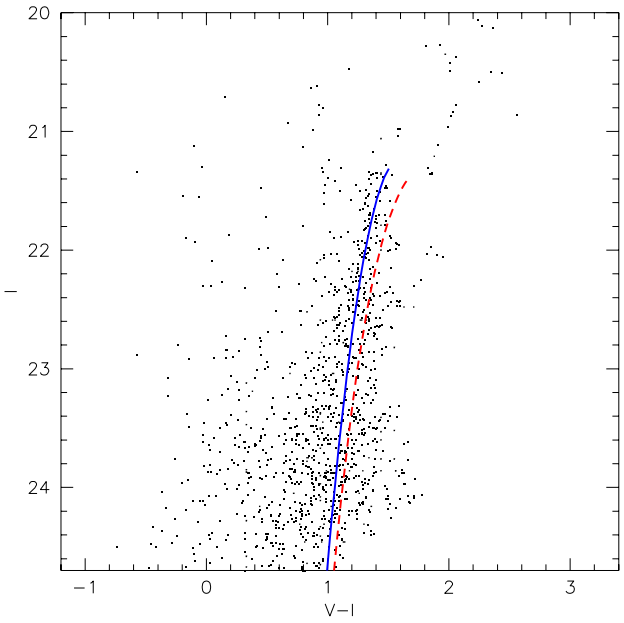

Fig. 3. The I, $(V-I)$ color-magnitude diagram of a sample of SagDIG stars with distance from the galaxy center $r > 0\farcm9$. The red giant stars in SagDIG are nearly as metal-poor as those in the Galactic globular cluster M 15 ([Fe/H]$=-2.17$, *solid line*), and more metal-poor than stars in M 2 ([Fe/H]$=-1.58$, *dashed line*). We use a distance modulus $(m-M) = 25.14$ and a reddening $E_{B-V} = 0.07$ for SagDIG.

The mean [Fe/H] of the "old" stellar population in SagDIG was estimated as in Saviane et al. (1996), by comparing the colors of the red giants with the RGB fiducial sequences of template Galactic globular clusters (GGC). The adopted reddening values are those specified above. The average color differences between the RGB stars in SagDIG and the GGC fiducials, measured in the interval $21.3 < I < 22.3$, were measured using the cluster ridge lines and metallicities of Da Costa & Armandroff (1990). A quadratic fit to the relation between mean color shifts and GGC metallicities yields [Fe/H]$=-2.08$ for SagDIG. The uncertainty, computed from the error on the color difference, is about 0.20 dex.

The metallicity obtained for SagDIG is among the lowest for dwarf galaxies, yet less extreme than found by previous authors. Had we adopted a reddening $E_{B-V} = 0.12$ (i.e. $E_{V-I} = 0.15$) as in KAM99, a mean [Fe/H]$= -2.31$ would have been obtained, which indicates that our metalliciy estimate and that of KAM99 are essentially consistent given the different assumption for the reddening. The

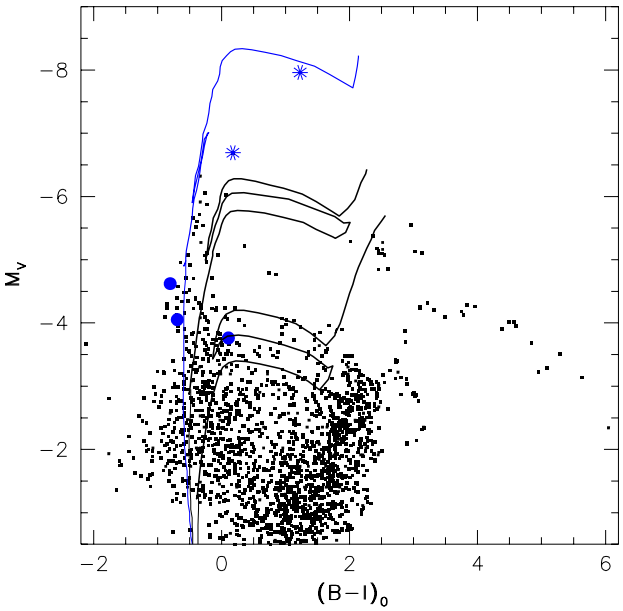

Fig. 4. The color-magnitude diagram of young stars in SagDIG, with superposed model isochrones with $Z = 0.0004$ and ages ∼10, 30, and 100 Myr (from Bertelli et al. 1994). We adopt a reddening $E_{B-V} = 0.19$, appropriate for the star-forming regions, and an apparent distance modulus 25.73. The *thin lines* represent the core H burning phase, while the *thick lines* represent the faster post-MS stages. Large filled circles represent three stars identified in the largest HII region, while the two starred symbols are objects coincident with the two smaller HII region candidates.

much lower metallicity range inferred by LK00 is most likely related to the photometric zero points adopted by these authors, yielding $(V - I)$ colors which are systematically bluer than those obtained by C87, KAM99, and this study.

5. Stellar populations

5.1. The recent star formation

Figure 4 shows a statistically cleaned color-magnitude diagram with superimposed a set of theoretical isochrones with ages 10, 30, and 100 Myr. The isochrones are $Z = 0.0004$ models ([Fe/H]=−1.7) from Bertelli's et al. (1994). A thick line emphasizes the He burning part of the isochrones. The CMD was transformed into the M_V, $(B - I)_0$ plane by adopting a true distance modulus 25.14 (see previous section) and a reddening appropriate for the star forming regions ($E_{B-V} = 0.19 \pm 0.05$, $A_V = 0.59 \pm 0.10$). The apparent distance modulus is therefore 25.73 mag.

The general picture of star formation is quite similar to that delineated by previous work. However, the cleaner CMD allowed by our statistical decontamination, together with the larger photometric baseline, provide new interesting pieces of information on the SFH of SagDIG. First, the blue-loops of the 30 Myr isochrone match quite well the luminosity and color of the two groups of blue and red stars near $M_V \simeq -5.5$. This supports the reality of the red group and its identification as a clump of red supergiants. According to the Padua models, such age implies a MS turnoff mass ∼ 9 $M_\odot$. Secondly, the blue stars in the range $-5 < M_V < -4$ appear perhaps too blue for $He-$burning stars, as KAM99 suggested – it is quite possible that they are MS stars slightly older than 10 million year. Further, we note the absence of a prominent plume of red supergiants that should be expected to define the red side of the blue loops. HST observations may eventually clarify this issue. Also, the obvious shortage of stars with age between 30 and 100 Myr suggests that the star formation rate dropped nearly 100 million years ago, with a short burst of star formation about 30 Myr ago interrupting a relatively quiescent period.

Table 3. Properties of stars projected onto the HII regions

region	star	x	y	V	$B-V$	$V-I$
SHK 1	12850	875.9	790.0	18.01	0.77	0.89
SHK 2	14120	859.9	869.8	19.28	0.14	0.47
SHK 3	12880	1182	792.5	21.35	−0.18	−0.19
SHK 3	12820	1166	788.1	22.21	0.05	0.49
SHK 3	13150	1185	809.6	21.92	−0.16	−0.10

Finally, we remark the presence of a few very bright stars spatially coincident with the candidate HII regions investigated by Strobel et al. (1991) (Table 3). Two bright objects ($M_V < -6$) were found in each of the two smaller candidate HII regions (#1 and #2). These objects have been classified as probably galactic, given the absence of [OIII] emission (Skillman et al. 1989b). The brightest one (in region SHK 1) is quite red, which is consistent with the identification with a foreground dwarf star. The color of the star coincident with region SHK 2 is consistent with a supergiant or a star clusters unresolved in ground-based data (see Cappellari et al. 1999). Three stars coincident in space with the bona-fide HII region (#3) are luminous and hot enough to represent possible exciting stars. They are as luminous as expected for ∼ 20 Myr main-sequence stars ($M_V \sim -4$, large circles in Fig. 4).

5.2. Spatial distributions: young stars vs. red giants

Stars of different ages in SagDIG are distributed in a very different way across the galaxy. Previous studies, starting with Cook (1987), had already noted that blue stars are only found in the central regions of SagDIG. In the following, we will show that the youngest stars are embedded in a region of high HI density, while the older populations are

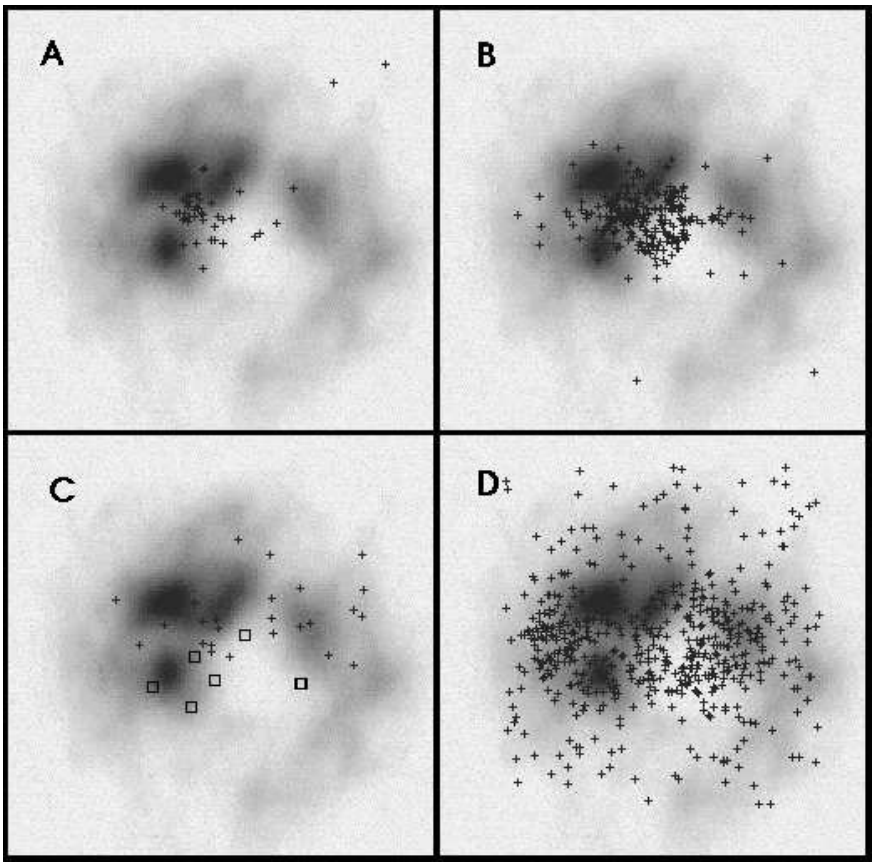

Fig. 5. The spatial distribution of young and old stars in SagDIG superimposed on the surface density map of HI from Young & Lo (1997). **a)** The most luminous blue stars in SagDIG, including both MS and BL stars; **b)** main sequence stars with age between 40 and 200 Myr; **c)** the carbon stars candidates from Cook (1987, *crosses*) and Demers & Battinelli (2001, *squares*); **d)** red giant branch stars as selected in Fig. 1. The field size of each panel is 8.5 arcmin. N is to the top, E to the left.

located away from the galaxy center, forming an extended halo or disk with a radial exponential fall-off.

Figure 5 shows the spatial distribution of stars in different age intervals, superimposed onto the surface density distribution of the neutral gas (from Young & Lo 1997). The latter authors showed that the ISM of SagDIG comprises a broad, warm component ($\sigma = 10$ km s^{-1}) and a narrow, cold one ($\sigma = 5$ km s^{-1}), with the warm component distributed throughout the galaxy (out to 3 Kpc from the center) while the cold one is concentrated into a small number of clumps of $\sim 8 \times 10^5$ $M_\odot$. A prominent clump is nearly coincident with the biggest HII region (Strobel et al. 1991).

The color and magnitude selections are those outlined in Fig. 1; no further statistical decontamination or spatial selection was applied. Two boxes sharing the color interval $-0.5 < B - I < 0.5$ were used to pick up MS stars approximately between $20 - 80$ Myr ($21.8 < V < 24.0$) and younger than 20 Myr ($19.4 < V < 21.8$), respectively. Both regions will also contain a fraction of He burning stars on the blue loops, somewhat older than MS stars at a given luminosity. For example, the blue stars in the brighter subsample are a mixture of MS stars younger than 20 Myr and He burning stars with age < 100 Myr.

The distributions of the young stars in both age intervals are plotted in Fig. 5*a* and *b*. The location of the youngest stars (panel *a*) indicates that the most recent star formation episode occurred in a small region located between the two brightest HI clumps along the gaseous shell, somewhat offset from the HI hole. The size of this association is $\sim 0\farcm5$ (180 pc).

The less young stars show a clumpy distribution around the same region, with a lower central concentration and a spatial extent of the order $2'$ in diameter (~ 600 pc). If we make the hypothesis that the young stars retain the velocity dispersion of the cold, dense HI clumps from which they probably originated, this size appears consistent with star diffusion in $\gtrsim 100$ Myr. Indeed, with a stellar velocity dispersion of about 5 km s^{-1}, equal to that of the narrow HI component (Young & Lo 1997), the crossing time of a 0.5 Kpc region is 100 Myr. Note, however, that the asymmetric shape of the star forming region in Fig. 5*b*, as well as the presence of several clumps in the distribution of young stars, suggest the occurrence of stochastic star formation associated with the HI shell. Probably what we are seeing is the result of a combination of the two mechanisms. We finally note that some blue stars are found in "tails", perhaps a hint of spiral structure, quite far from the main star-forming site. This may be the signature of star formation on the rim of the shell.

In contrast to the distribution of the young stars, the red giants in SagDIG are uniformly distributed across the galaxy (Fig. 5*d*), with their mean position approximately coincident with that of the blue stars. Interestingly, we note a degree of coincidence with the ridges and arms in the distribution of neutral gas, which appears more than fortuitous – e.g., note the arm-like filaments of stars tracing the western rim of the HI shell. These red stars need

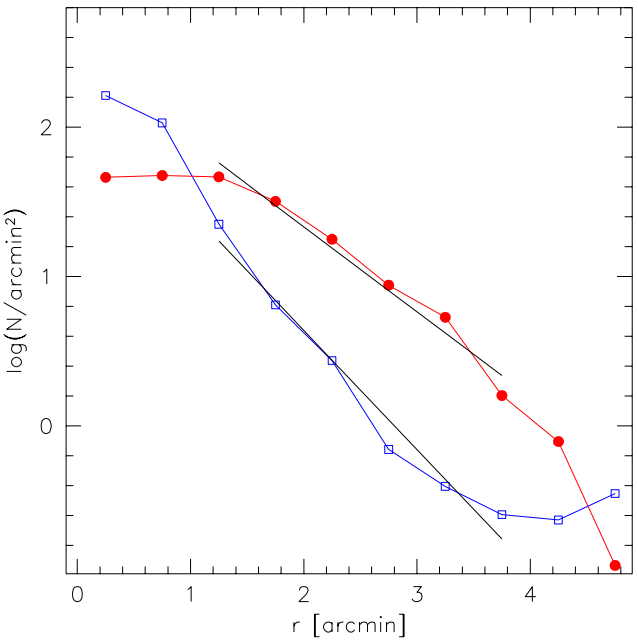

Fig. 6. The surface density profiles of young stars (*open squares*) and red giant stars (*filled circles*) in SagDIG. The straight lines represent exponential fits to the density distribution of young and old stars. Note the larger scale length of the extended halo of red stars surrounding the inner, star-forming regions of SagDIG.

not be very old: they may well be relatively young red giants (yet older then 1 Gyr), as it is probably the case in Leo A (Tolstoy et al. 1998). The intermediate-age upper-AGB population seems to share the extended distribution of the red giants, as it can be seen from the distribution of C stars in the samples of Cook (1987) and Demers & Battinelli (2001) (Fig. 5*c*).

Figure 6 shows the different surface density profiles of blue stars (younger than about 80 Myr; $19.4 < V < 24.0$) and red giants. The profiles are plotted against the distance from the galaxy center, defined as the mean x, y of red giants. Both profiles are nearly exponential as expected in dwarf galaxies. It is apparent from this figure that the radial scale length of the RGB stars is larger than for the blue stars. A linear fit in the radial range $1\farcm2 < r < 3\farcm8$ (0.4–1.2 Kpc) provides a quantitative estimation of the different exponential scale lengths of young and "old" stars. The scale lengths are $46''$ and $33''$ (0.24 and 0.17 Kpc) for the red giants and blue stars, respectively. The global scale lengths measured by KAM99 and LK00 are clearly dominated by the young stars. The central flattening of the RGB star profile is quite uncertain in the innermost 0.3 Kpc, because of incompleteness in the star counts caused by the extreme crowding. In particular, the red stars are likely to be masked by the more luminous young star complexes. Overall, there are several hints that SagDIG may be a disk galaxy seen nearly face-on, owing its irregular shape to the optical signatures of recent star formation. The rotation required to support such a low-mass galaxy is very small, and could easily be masked by the turbulent gas motions (see Young & Lo 1997).

5.3. The metallicity-luminosity relation

The metallicity estimated in Sect. 4.2 for the red giant stars in SagDIG ([Fe/H]$\simeq -2.1$) turns out to be in good agreement with the metal content estimated for the ISM. A new determination of the oxygen abundance in the HII regions of SagDIG is presented in a companion paper (Saviane et al. 2001). The new estimate, $12+\log(\mathrm{O/H}) = 7.23\pm0.20$, revises downwards the [O/H] determination of Skillman et al. (1989b), yielding (under the same physical assumptions) a value more metal-poor by about 0.2 dex. We have transformed this result to [Fe/H]$=-2.07\pm0.20$ by adopting $12+\log(\mathrm{O/H})_{\odot} = 8.93$ for the solar O abundance, and using the mean difference between [Fe/H] and [O/H] given by Mateo (1998). Under these assumptions, the composition of the warm gas in the HII regions does not appear to be significantly metal enriched with respect to the red giant stars.

These new estimates of the mean metallicity of both the red giant star population and the warm ISM in SagDIG are compared with the properties of other dwarfs in the metallicity–luminosity diagram. Figure 7 shows a plot of both stellar [Fe/H] and nebular [O/H] measurements (see Skillman et al. 1989a) against luminosity for a large sample of dwarf galaxies. The SagDIG data point was plotted using our estimates of mean metallicity and the M_V measured by KAM99. The data are mostly from Mateo (1998) and van den Bergh (2000). SagDIG now appears to be consistent with the general trend of metallicity against luminosity for dwarf irregulars. Its metallicity, although less extreme than found by previous studies, remains the lowest among Local Group galaxies, and shares the tendency of low-luminosity dIrrs (e.g., UKS 2323-326: Lee & Byun 1999; WLM: Minniti & Zijlstra 1997; Sextans A: van Dyk et al. 1998) to a lower stellar metallicity than dSph galaxies of comparable luminosities. Whether this trend is really produced by a bimodal metallicity, or rather is due to the fact that RGB stars may have a younger age in dIrrs than in dwarf spheroidals, is still matter of debate.

6. Summary and conclusions

We have presented a *BVI* study of the stellar content and metallicity of UKS 1927-177, the Sagittarius dwarf irregular galaxy, based on deep color-magnitude diagrams.

We have found that *the color-magnitude diagram of SagDIG is better understood by introducing a differential reddening scenario* in which the young stars, located near high-density HI clumps, are more reddened than the older stars distributed all over the galaxy. In fact, the color distribution of the Galactic foreground stars indicates a relatively low reddening (we assume $E_{B-V} = 0.07\pm0.02$ for the old stars), while measurements of the Balmer decrement in HII regions (Skillman et al. 1989b; Saviane et al.

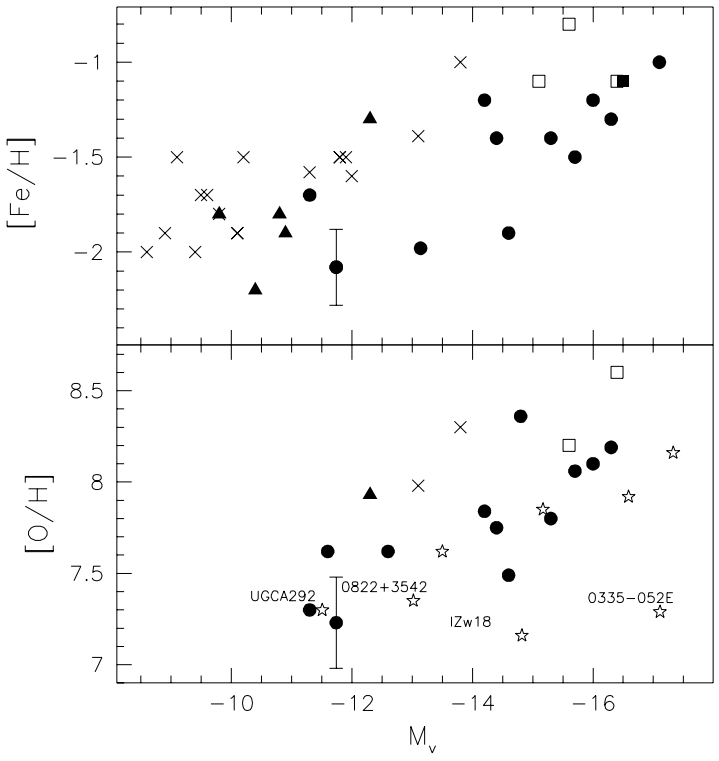

Fig. 7. Metallicities of stars and the ISM of dwarf galaxies in the Local Group and beyond, plotted against their V absolute magnitude. References to data are given in the text. *Upper panel: crosses* refer to dSph galaxies, *open squares* are the dE companions to M 31, the *filled square* is the data point for the low-luminosity elliptical M 32, *filled circles* are dwarf irregulars, and *triangles* represent "transition" galaxies (dSph/dI) (see Mateo 1998). SagDIG is represented by the data point with error bars. *Lower panel:* The [O/H] abundances of the gaseous component, measured from nebular emission lines. The symbols are the same as for the stellar metallicities. *Stars* represent dwarf irregulars or blue compact dwarfs outside the Local Group.

2001) provide a higher reddening, $E_{B-V} = 0.19$. Using the lower reddening for the "old" population in SagDIG, we obtained revised values for the metallicity and distance, [Fe/H]$= -2.1 \pm 0.2$ and $(m - M)_0 = 25.14 \pm 0.18$, respectively. While the distance confirms previous estimates, *our metallicity turns out to be significantly higher* than those proposed by Karachentsev et al. (1999) and Lee & Kim (2000). *Using this new metallicity, we have compared SagDIG with other dwarf galaxies in the luminosity-metallicity diagram, and found that it is consistent with the general trend for dIrr galaxies.*

The large baseline given by the $(B-I)$ color, together with an analysis based on statistical subtraction of the Galactic foreground, provided additional information on the recent star formation in SagDIG. The C stars from two sources have also been compared with our cleaned CMDs, which confirmed the presence of an intermediate age population. For the young stellar population, we have adopted the reddening derived for the HII regions, thus obtaining a good match to the theoretical isochrones. A comparison with models indicates a significant burst taking place ∼30 Myr ago, with star formation going on until ∼10 Myr ago. This burst seems to have interrupted a relatively quiescent period between ∼30–100 Myr ago. We identified a group of candidate red supergiants that are quite well fitted by the isochrones of young He-burning stars.

We have also obtained a detailed quantitative comparison of *the spatial distribution of stars in different age ranges* with the distribution of the ISM. Different density profile scale lengths have been measured for the young blue stars and the red giants. The youngest stars have been shown to concentrate in a central region nearly coincident with the density peaks in the HI distribution. In constrast, the distribution of red giants is quite extended, yet it seems to be correlated with the HI morphology as well. This may suggest for the red giants in SagDIG a contribution by relatively young (a few Gyr old) stars. We also noted that some blue stars are found in "tails", perhaps a hint of spiral structures, quite far from the main star-forming sites. This suggests a similarity with the small spiral-like structures that can form even in a small galaxy according to the theory of stochastic self-propagating star formation (Gerola & Seiden 1978). An alternative possibility is that these features are a vestige of star formation related to the gaseous shell.

Acknowledgements. We thank F. Bresolin for useful comments on an early draft, and the anonymous referee for helpful remarks that improved the presentation of this paper. This research has made use of the NASA/IPAC Extragalactic Database (NED) and of NASA's Astrophysics Data System Service.

References

Bellazzini, M., Ferraro, F. R., Pancino, E. 2001, ApJ, in press
Bertelli, G., Bressan, A., Chiosi, C., Fagotto, F., & Nasi, E. 1994, A&AS, 106, 275

Burstein, D., & Heiles, C. 1984, ApJS, 54, 33
Caldwell, J. A. R., & Schecter, P. L. 1996, AJ, 112, 772
Calzetti, D., Kinney, A. L., & Storchi-Bergmann, T. 1994, ApJ, 429, 582
Cappellari, M., Bertola, F., Burstein, D., Buson, L. M., Greggio, L., & Renzini, A. 1999, ApJL, 515, L17
Cesarsky, D. A., Laustsen, S., Lequeux, J., Schuster, H.-E., & West, R. M. 1977, A&A, 61, L31
Cook, K. H. 1987, PhD Thesis, Univ. Arizona (C87)
Da Costa, G. S., & Armandroff, T. E. 1990, AJ, 100, 162 (DA90)
Demers, S., & Battinelli, P. 2001, AJ, in press (astro-ph/0109512)
Gerola, H., & Seiden, P. 1978, ApJ, 223, 129
Held, E. V., Saviane, I., & Momany, Y. 1999, A&A, 345, 747
Karachentsev, I., Aparicio, A., & Makarova, L. 1999, A&A, 352, 363
Landolt, A. U. 1992, AJ, 104, 340
Lee, M. G. & Byun, Y. 1999, AJ, 118, 817
Lee, M. G., Freedman, W. L., & Madore, B. F. 1993, ApJ, 417, 553
Lee, M. G. & Kim, S. C. 2000, AJ, 119, 777
Lo, K. Y., Sargent, W. L., & Young, K. 1993, AJ, 106, 507
Longmore, A. J., Hawarden, T. G., Webster, B. L., Goss, W. M., & Mebold, U. 1978, MNRAS, 183, 97P
Madore, B. F. & Freedman, W. L. 1995, AJ, 109, 1645
Mateo, M. 1998, ARA&A, 36, 435
Minniti, D., & Zijlstra, A. A. 1997, AJ, 114, 147
Mould, J. R., & Kristian, J. 1986, ApJ, 305, 591
Pritchet, C. J., & van den Bergh, S. 1999, AJ, 118, 883
Sakai, S., Madore, B. F., & Freedman, W. L. 1999, ApJ, 511, 671
Salaris, M., Cassisi, S. 1998, MNRAS, 298, 166
Saviane, I., Held, E. V., & Piotto, G. 1996, A&A, 315, 40
Saviane, I., Held, E. V., & Bertelli, G. 2000, A&A, 355, 56
Saviane, I., Rizzi, L., Held, E. V., Bresolin, F., & Momany, Y. 2001, A&A, submitted
Schlegel, D. J., Finkbeiner, D. P., & Davis, M. 1998, ApJ, 500, 525
Seaton, M. J. 1979, MNRAS, 187, 73
Skillman, E. D., Kennicutt, R. C., & Hodge, P. W. 1989a, ApJ, 347, 875
Skillman, E. D., Terlevich, R., & Melnick, J. 1989b, MNRAS, 240, 563
Stetson, P. B. 1987, PASP, 99, 191
Stetson, P. B. 1994, PASP, 106, 250
Strobel, N. V., Hodge, P., & Kennicutt, R. C. J. 1991, AJ, 383, 148
Tolstoy, E., Gallagher, J.S., Cole, A.A., et al. 1998, AJ, 116, 1244
van den Bergh, S. 1994, AJ, 107, 1328
van Dyk, S. D., Puche, D., & Wong, T. 1998, AJ, 116, 2341
van den Bergh, S. 2000, PASP, 112, 529
Young, L. M., & Lo, K. Y. 1997, ApJ, 490, 710
Zijlstra, A. A., & Minniti, D. 1999, AJ, 117, 1743